

1 **Retrograde suppression of post-tetanic potentiation at the mossy fiber-CA3
2 pyramidal cell synapse**

4 **Abbreviated Title:** Activity-dependent suppression of PTP

6 Sachin Makani^{1#}, Stefano Lutzu^{1#}, Pablo J. Lituma^{1#}, David L. Hunt^{1,3}, and Pablo E. Castillo^{1,2*}

8 ¹Dominick P. Purpura Department of Neuroscience, Albert Einstein College of Medicine, Bronx,
9 NY 10461

10 ² Department of Psychiatry and Behavioral Sciences, Albert Einstein College of Medicine,
11 Bronx, NY 10461.

12 ³ Current address: Center for Neural Science and Medicine, Cedars-Sinai Medical Center, Los
13 Angeles, CA 90048

15 [#]Equal contribution

17 **Author Contributions:** SM, SL, PJL and PEC designed the experiments. SM, SL and PJL
18 performed experiments and analyzed data. DLH performed preliminary experiments and made
19 observations that triggered this study. SM and PEC wrote the first manuscript which was edited
20 by all authors.

22 ***Correspondence should be addressed to:**

23 Pablo E. Castillo, M.D., Ph.D.
24 Dominick P. Purpura Department of Neuroscience
25 Albert Einstein College of Medicine
26 Rose F. Kennedy Center, Room 703
27 1410 Pelham Parkway South
28 Bronx, NY 10461
29 Phone: 718.430.3262
30 E-mail: pablo.castillo@einsteinmed.org

33 Number of Figures: 6
34 Number of Tables: none
35 Number of Multimedia: none
36 Number of Extended Figures: 2

Number of words for Abstract: 177
Number of words for Significant Statement: 119
Number of words for Introduction: 388
Number of words for Discussion: 1334

39 **Funding sources:** This work supported by the NIH (F32-NS077696 to S.M.; R01-DA17392, R01
40 MH116673 and NIH R01MH125772 to P.E.C.). S.M. was partially supported by T32-NS007439.

42 **Acknowledgements:**

43 We thank all the Castillo lab members for invaluable discussions. We also thank Professor
44 Peter Jonas for his insightful comments on a recent version of our manuscript.

46 **Conflict of Interest:** There are no conflicts of interest to report.

1 **ABSTRACT**

2 In the hippocampus, the excitatory synapse between dentate granule cell axons – or mossy
3 fibers (MF) – and CA3 pyramidal cells (MF-CA3) expresses robust forms of short-term plasticity,
4 such as frequency facilitation and post-tetanic potentiation (PTP). These forms of plasticity are
5 due to increases in neurotransmitter release, and can be engaged when dentate granule cells
6 fire in bursts (e.g. during exploratory behaviors) and bring CA3 pyramidal neurons above
7 threshold. While frequency facilitation at this synapse is limited by endogenous activation of
8 presynaptic metabotropic glutamate receptors, whether MF-PTP can be regulated in an activity-
9 dependent manner is unknown. Here, using physiologically relevant patterns of mossy fiber
10 stimulation in acute mouse hippocampal slices, we found that disrupting postsynaptic Ca^{2+}
11 dynamics increases MF-PTP, strongly suggesting a form of Ca^{2+} -dependent retrograde
12 suppression of this form of plasticity. PTP suppression requires a few seconds of MF bursting
13 activity and Ca^{2+} release from internal stores. Our findings raise the possibility that the powerful
14 MF-CA3 synapse can negatively regulate its own strength not only during PTP-inducing activity
15 typical of normal exploratory behaviors, but also during epileptic activity.

16

17 **SIGNIFICANCE STATEMENT**

18 The powerful mossy fiber-CA3 synapse exhibits strong forms of plasticity that are engaged
19 during location-specific exploration, when dentate granule cells fire in bursts. While this synapse
20 is well-known for its presynaptically-expressed LTP and LTD, much less is known about the
21 robust changes that occur on a shorter time scale. How such short-term plasticity is regulated,
22 in particular, remains poorly understood. Unexpectedly, an *in vivo*-like pattern of presynaptic
23 activity induced robust post-tetanic potentiation (PTP) only when the postsynaptic cell was
24 loaded with a high concentration of Ca^{2+} buffer, indicating a form of Ca^{2+} -dependent retrograde
25 suppression of PTP. Such suppression may have profound implications for how environmental
26 cues are encoded into neural assemblies, and for limiting network hyperexcitability during
27 seizures.

28

1 **INTRODUCTION**

2

3 Mossy fibers (MFs), the axonal projections of dentate granule cells (GC), provide a strong
4 excitatory input onto hippocampal CA3 pyramidal neurons (Henze et al., 2000; Nicoll and
5 Schmitz, 2005). The MF-CA3 synapse is well known for exhibiting uniquely strong forms of
6 short-term potentiation, including paired-pulse facilitation (PPF) and frequency facilitation, which
7 last milliseconds to seconds (Salin et al., 1996). More intense periods of high-frequency
8 stimulation typically elicit post-tetanic potentiation (e.g. MF-PTP), which decays over several
9 minutes (Griffith, 1990). These forms of plasticity are commonly attributed to an increase in
10 presynaptic release probability (Pr) (Zucker and Regehr, 2002; Nicoll and Schmitz, 2005;
11 Regehr, 2012), a change in the readily releasable pool (Vandael et al., 2020), and transiently
12 convert the synapse from a high- to lower-pass filter (Abbott and Regehr, 2004). In behaving
13 rodents, during place field activation, GCs can fire in high-frequency bursts (Pernia-Andrade
14 and Jonas, 2014; Diamantaki et al., 2016; GoodSmith et al., 2017; Senzai and Buzsaki, 2017),
15 driving CA3 pyramidal neurons above threshold (Henze et al., 2002). Thus, frequency
16 facilitation and MF-PTP could have a profound impact on how memory traces are encoded into
17 CA3 neural ensembles.

18

19 Given the apparent ease with which these robust forms of presynaptic potentiation are elicited
20 at the MF-CA3 synapse, one might expect a process by which the connection is negatively
21 regulated. In fact, there is evidence that endogenously released glutamate transiently
22 suppresses frequency facilitation via presynaptic group II metabotropic glutamate receptors (II-
23 mGluRs) (Scanziani et al., 1997; Toth et al., 2000; Kwon and Castillo, 2008a). It is unknown,
24 however, whether forms of longer-lasting plasticity, such as MF-PTP, are also curtailed in an
25 activity-dependent manner.

26

1 In the present study we performed whole-cell recordings from CA3 pyramidal neurons in mouse
2 hippocampal slices and mimicked physiologically-relevant activity patterns by stimulating GCs
3 with a brief, high-frequency bursting paradigm. To our surprise, MF-PTP was readily observed
4 when the postsynaptic cell was dialyzed with a solution containing high Ca^{2+} buffering
5 properties, but was nearly absent when the recording solution had a lower, more physiological
6 Ca^{2+} buffering capacity. These findings strongly suggest that MF-PTP is normally suppressed by
7 a Ca^{2+} -dependent retrograde mechanism. Such negative feedback could not only enable
8 homeostatic regulation of MF-CA3 synaptic strength, ensuring that the essential filtering
9 properties of the connection are maintained during ongoing activity, but also prevent runaway
10 network excitability, as may occur during epileptic activity.

11

12 **METHODS**

13

14 **Slice Preparation**

15 Animal procedures were approved by our Institutional Animal Care and Use Committee and
16 adhered to National Institutes of Health guidelines. C57BL mice (18-28 days old) were deeply
17 anesthetized with isoflurane, decapitated, and brains rapidly removed and both hippocampi
18 were dissected. Transverse hippocampal slices (400 μm) were cut on a DTK-2000 microslicer
19 (Dosaka, Kyoto, Japan) or a Leica VT1200 S vibratome, in ice-cold cutting solution containing
20 (in mM): 215 sucrose, 2.5 KCl, 20 glucose, 26 NaHCO_3 , 1.6 NaH_2PO_4 , 1 CaCl_2 , 4 MgSO_4 , and 4
21 MgCl_2 . After 10 minutes of incubation at room temperature, the cutting solution was exchanged
22 for the artificial cerebrospinal fluid (ACSF) containing 124 NaCl , 2.5 KCl, 10 glucose, 26
23 NaHCO_3 , 1 NaH_2PO_4 , 2.5 CaCl_2 , and 1.3 MgSO_4 . Both cutting and ACSF solutions were
24 saturated with 95% O_2 and 5% CO_2 (pH 7.4). The slices recovered at room temperature for at
25 least 1.5 hour before recording.

26

1 **Electrophysiology**

2 Slices were transferred to a recording chamber and perfused with ACSF (2 ml/min). Recordings
3 were done at 25°C, except for the experiments included in **Fig 1a, 6e-h**, and those that used
4 BoTX that were performed at 32°C. The recording pipette was filled with an internal solution
5 containing (in mM): 112 K-gluconate, 17 KCl, 0.04 CaCl₂, 10 HEPES, 2 Mg-ATP, 0.2 GTP, 10
6 NaCl, and 0.1 EGTA (pH 7.2) (290–295 mOsm). For the experiments using 10 mM EGTA or
7 BAPTA, the concentration of K-gluconate was reduced to compensate for osmolarity. The
8 pipette resistance ranged from 3–4 MΩ. Series resistance (6–15 MΩ) was monitored throughout
9 the experiment, and those experiments in which the series resistance changed by more than
10 10% were not included for analysis. Patch pipettes were pulled on a PP-830 vertical puller
11 (Narishige, Tokyo, Japan).

12

13 Responses were generated by stimulating presynaptic axons and recording from CA3 pyramidal
14 neurons. Kainate receptor (KAR) responses were recorded in the presence of GYKI-53655 (30
15 μM) or LY 303070 (15 μM), and CGP-55845 (3 μM) in the bath, and MK-801 (2 mM) in the
16 pipette. With the exception of data obtained in **Fig. 1a**, **Extended Fig. 5c** and **Fig. 6e-h**, α-
17 amino-3-hydroxy-5-methyl-4-isoxazole propionic acid receptor (AMPAR)-mediated responses
18 were also generated with MK-801 in the pipette, and GYKI-53655 (1 μM) in the bath (Kwon and
19 Castillo, 2008a). N-methyl-D-aspartate receptor (NMDAR) responses were recorded with NBQX
20 (10 μM) in the bath. All experiments except those in **Fig. 1a,c** and **Fig. 6e-h** contained
21 picrotoxin (100 μM).

22

23 KAR and NMDAR-mediated EPSCs were evoked by placing a monopolar stimulating pipette
24 with a broken tip (~5–10 μm diameter, filled with ACSF) in the dentate gyrus (DG) cell body
25 layer. For AMPAR-mediated responses, the tip was left unbroken (~1 μm) to minimize the
26 number of MFs activated. For minimal stimulation experiments, a theta-glass stimulating pipette

1 was placed in stratum lucidum 100 μ m apart from the recorded CA3 pyramidal cell. Intensity
2 was increased until a success/failure pattern of AMPAR-EPSC responses was observed. MF
3 AMPAR-EPSCs were only accepted for analysis if the following criteria were met: robust PPF
4 (at least 2 fold), DCG-IV sensitivity > than 85%, fast rise time (10-90%) was < 1.2 ms, response
5 onset was < 5.0 ms, and these values did not significantly change after the bursting. These
6 criteria were based on those established by previous studies of MF-CA3 transmission (Jonas et
7 al., 1993). To record KAR- and AMPAR-EPSCs, cells were voltage-clamped at -60 mV. For
8 NMDAR-EPSCs, cells were held at -50 mV. Unless otherwise stated, baseline NMDAR- and
9 KAR-EPSCs were obtained by delivering two stimuli separated by 5 ms in order to evoke a
10 measurable response (Weisskopf and Nicoll, 1995). Stimulus intensity for KAR/NMDAR- and
11 AMPAR-mediated responses was approximately 100 and 10 μ A, respectively. Stimulus
12 intensities did not differ, on average, between control and BAPTA-dialyzed cells in any given
13 condition. Stimulus duration was 100-200 μ s. CA3 neurons were always dialyzed for \geq 15 min,
14 while stimulating at 0.1 Hz, before delivering any plasticity-inducing stimulation. For synaptically-
15 evoked action potentials (**Fig. 6e-h**), no drugs were bath applied and CA3 pyramidal cells were
16 held in current-clamp mode before, during and after the induction. Resting potential was kept
17 between -70 and -75 mV. Baseline and post-induction spiking probability were measured as the
18 average of number of spikes per burst normalized to the number of pulses per burst. (i.e. 3
19 pulses at 25 Hz).

20

21 The baseline stimulation frequency for all experiments was 0.1 Hz, except for frequency
22 facilitation (5 stimuli, 25 Hz), which was delivered at 0.05 Hz. The standard PTP induction
23 protocol consisted of 25 bursts (5 stimuli, 50 Hz) delivered at 2 Hz. PTP was never generated
24 more than once in a given slice. To achieve a similar time course of potentiation in BAPTA-
25 dialyzed cells when the inter-stimulus interval was 40 ms (**Fig. 3c**), or when monitoring MF
26 AMPAR-mediated transmission (**Figs. 1a, 3b**), it was necessary to use 50 bursts. The bursting

1 protocol was delivered while cells were voltage-clamped at -60 mV, except for one experiment
2 in which the induction was performed in current-clamp (**Fig. 1a,c** and **Fig. 6e-h**). Long-term
3 potentiation (LTP) in CA1 pyramidal neurons was induced by pairing postsynaptic depolarization
4 from -60 mV to 0 mV for 3 min with low-frequency stimulation of Schaffer collaterals (180
5 pulses, 2 Hz).

6

7 In all experiments examining MF synaptic transmission, the mGluR2/3 agonist DCG-IV (1-2 μ M)
8 was applied at the end of the experiment and data were included only when the response was
9 inhibited by more than 85%. For perforated patch experiments, nystatin was first dissolved into
10 DMSO (10 mg/mL). This was then diluted 250-fold into the intracellular solution to yield 40
11 μ g/mL. Botulinum toxin-B (BoTX) was prepared by making a 0.5 μ M stock solution with 1
12 mg/mL BSA. This was then diluted 100-fold into the final intracellular solution, with 0.5 mM DL-
13 Dithiothreitol (DTT).

14

15 **Reagents**

16 MK-801, NBQX, CGP-55845, Nimodipine, AM-251, DCG-IV, and GYKI 53655 were obtained
17 from Tocris-Cookson (Minneapolis, MN, USA). LY 303070 was obtained from ABX advanced
18 biochemical compounds (Radeberg, Germany). BoTX was obtained from List Biological
19 (Cambell, CA, USA). All other chemicals and drugs were purchased from Sigma-Aldrich (St.
20 Louis, MO, USA).

21

22 **Data Analysis**

23 Experiments were executed with a MultiClamp 700B amplifier (Molecular Devices, Union City,
24 CA, USA). Data were analyzed online using IgorPro (Wavemetrics, Lake Oswego, OR, USA),
25 and offline with Origin 9.2 (Northampton, MA, USA) and GraphPad Prism (La Jolla, CA, USA).
26 The three minutes before the induction protocol was used as a baseline for statistics. Following

1 the protocol, the first three minutes were used to calculate PTP, and the last three minutes (of a
2 30 minute period) for the positive control experiment testing LTP at the Schaffer collateral to
3 CA1 pyramidal cell synapse (**Extended Fig. 5c**). Representative responses are averages of 18
4 traces. All values are shown as mean \pm SEM. Unless otherwise stated, Student's t-test was
5 used for statistical significance between two samples, and ANOVA for multiple comparisons.
6 Data that did not display a normal distribution were compared using the non-parametric test
7 Mann-Whitney. All experiments for a given condition were performed in an interleaved fashion –
8 i.e. control experiments were performed for every test experiment.

9

10

11 **RESULTS**

12

13 **Mossy fiber post-tetanic potentiation is minimal under physiological postsynaptic Ca^{2+} 14 buffering conditions**

15

16 This study was initiated by the unexpected observation that MF-PTP magnitude was highly
17 dependent on the postsynaptic Ca^{2+} buffering conditions. We induced MF-PTP by activating
18 MFs with a bursting protocol (25 bursts delivered at 2 Hz; 5 stimuli at 50 Hz within a burst)
19 designed to mimic physiological activity patterns of GCs *in vivo* (Henze et al., 2002; Pernia-
20 Andrade and Jonas, 2014; Diamantaki et al., 2016; GoodSmith et al., 2017; Senzai and
21 Buzsaki, 2017), while monitoring AMPAR-EPSCs (see Methods) under physiological recording
22 conditions –e.g. no drugs in the bath, near-physiological recording temperature (32°C) and
23 voltage clamping at resting membrane potential (chloride reversal potential). The PTP induction
24 protocol was delivered in current-clamp configuration so that CA3 cells were able to fire freely.
25 To our surprise, we did not observe much potentiation when postsynaptic CA3 pyramidal cells
26 were loaded with 0.1 mM EGTA, a near physiological intracellular Ca^{2+} buffering condition that

1 we refer as “control”, but saw robust MF-PTP with 10 mM BAPTA in the postsynaptic pipette
2 (**Fig. 1a**). In contrast, BAPTA did not increase PTP of associational-commissural (AC) synaptic
3 responses (**Fig. 1b**). These results are consistent with previous studies that reported little
4 potentiation at the AC synapse (Salin et al., 1996), and suggest that the robust PTP unmasked
5 in BAPTA-dialyzed cells is specific to the MF-CA3 synapse. Importantly, the enhancement of
6 MF-PTP under high postsynaptic Ca^{2+} buffering conditions was also observed with minimal
7 stimulation of MFs (Jonas et al., 1993) (**Fig. 1c**), indicating that the PTP enhancement is not an
8 artifact due to strong extracellular stimulation. Lastly, we found that 10 mM BAPTA did not affect
9 the basal paired-pulse ratio (PPR) (i.e. prior to bursting) (**Fig. 1d**), making unlikely that changes
10 in basal Pr could account for the PTP enhancement. These initial observations suggested that
11 MF-PTP, a phenomenon widely believed to be presynaptic in nature, was under the control of a
12 postsynaptic Ca^{2+} -dependent process that deserved further investigation.

13
14 A major problem when studying MF-CA3 synaptic plasticity is the polysynaptic contamination
15 associated with extracellular stimulation of MFs (Claiborne et al., 1993; Henze et al., 2000;
16 Nicoll and Schmitz, 2005; Kwon and Castillo, 2008a). Repetitive stimulation aggravates this
17 problem as MF-CA3 synapses can be potentiated several-fold by strong frequency facilitation
18 (Regehr et al., 1994; Salin et al., 1996). To rule out the possibility that the PTP was the result of
19 polysynaptic contamination, we blocked AMPA and NMDA receptor-mediated transmission, and
20 monitored kainate receptor-EPSCs (KAR-EPSCs), which are observed at MF-CA3 synapses but
21 not AC-CA3 synapses (Castillo et al., 1997). When CA3 pyramidal neurons were loaded with 10
22 mM BAPTA the burst stimulation protocol caused a robust PTP of KAR-mediated transmission
23 as compared to control (0.1 mM EGTA) (**Fig. 2a**). To discard that PTP suppression could be
24 due to some unexpected effect of BAPTA, we repeated our experiments with 10 mM EGTA, a
25 slow Ca^{2+} chelator that is widely used at this concentration in voltage-clamp recordings. MF-
26 PTP was equally robust in 10 mM EGTA-loaded cells (**Fig. 2b, Extended Fig. 2**). To ensure

1 fast postsynaptic Ca^{2+} chelation, subsequent experiments compared cells loaded with 0.1 mM
2 EGTA vs. 10 mM BAPTA. Collectively, these findings demonstrate that postsynaptic Ca^{2+}
3 buffering had a striking influence on the magnitude of MF-PTP.

4

5 One interpretation of the set of observations above is that CA3 pyramidal neurons normally
6 have high Ca^{2+} buffering capacity (i.e. similar to 10 mM EGTA), and replacing these with the 0.1
7 mM EGTA solution somehow abolished PTP. To directly address this possibility, we monitored
8 KAR-EPSPs with BAPTA in the recording pipette, in perforated patch vs. whole-cell
9 configuration. In perforated patch conditions, in which BAPTA could not diffuse into the cell, only
10 a small amount of PTP was seen, while KAR-EPSPs in whole-cell mode displayed similar
11 striking potentiation observed above when KAR-EPSCs were recorded from BAPTA-loaded
12 cells (**Fig. 2c**, see also **Fig. 2a**). These results indicate that the endogenous Ca^{2+} buffering
13 capacity of CA3 pyramidal neurons was functionally more similar to the 0.1 mM EGTA solution
14 than to the 10 mM BAPTA solution.

15

16 We next confirmed the presynaptic nature of MF-PTP in BAPTA conditions. If this PTP was
17 presynaptic, it should be similarly observed when monitoring KAR-EPSCs, NMDAR-EPSCs and
18 AMPAR-EPSCs (unlike the data reported in **Fig. 1a**, AMPAR-EPSCs in these experiments were
19 pharmacologically isolated and recorded under conditions of low network excitability; see
20 Methods). Indeed, when either NMDAR- or AMPAR-mediated EPSCs were monitored, little to
21 no potentiation was observed in control conditions, but the response was markedly increased in
22 BAPTA (**Fig. 3a,b**). Notably, there was no difference when comparing the PTP magnitude of
23 control cells in KA, AMPA, and NMDA receptor groups to each other (ANOVA; $F=1.76$; $p>0.2$,
24 $DF=15$), or when comparing the BAPTA-dialyzed cells in the three receptor groups to each
25 other (ANOVA; $F=0.74$; $p>0.4$, $DF=17$). Thus, the difference in PTP between control and
26 BAPTA persisted regardless of which postsynaptic receptor was pharmacologically isolated. To

1 assess changes in PPR, we monitored KAR-mediated responses. Here, the induction was
2 accompanied by a greater reduction in PPR in BAPTA-dialyzed cells, consistent with an
3 increase in Pr. Importantly, in both control and BAPTA-dialyzed cells, the recovery time course
4 of EPSC amplitude and PPR mirrored each other (**Fig. 3c**), suggestive of a causal relationship
5 between presynaptic Pr and the postsynaptic response magnitude. Together, these
6 independent lines of evidence confirm a presynaptic locus of MF-PTP in BAPTA-dialyzed cells.
7 Again, as for AMPAR-EPSCs (**Fig. 1d**), no significant difference was noted in the degree of
8 basal PPR (i.e. before bursting) between control and BAPTA-dialyzed cells (Control: 2.4 ± 0.2 ;
9 $n=25$; BAPTA 2.7 ± 0.2 ; $n=27$; Control vs. BAPTA $p>0.2$; data not shown), supporting the notion
10 that postsynaptic BAPTA loading did not affect basal Pr. The most parsimonious explanation for
11 a robust presynaptic potentiation being unmasked by preventing a rise in postsynaptic Ca^{2+} is a
12 retrograde signal that suppresses potentiation in normal conditions. This interpretation is
13 consistent with the fact that most forms of retrograde signaling so far described require a rise in
14 postsynaptic Ca^{2+} concentration (Fitzsimonds and Poo, 1998; Regehr et al., 2009).

15

16 **Source of postsynaptic Ca^{2+} rise involved in PTP suppression**

17 We next sought to assess the source or sources of the postsynaptic Ca^{2+} rise involved in the
18 suppression of MF-PTP. Ca^{2+} influx via NMDARs, or Ca^{2+} -permeable AMPARs or KARs, was
19 ruled out as solely sufficient for retrograde suppression, given that pharmacological blockade of
20 these receptors did not unmask PTP (**Figs. 2, 3a**). Several voltage-gated Ca^{2+} channels
21 (VGCCs) exist in the thorny excrescence of CA3 pyramidal neurons (Kapur et al., 2001; Reid et
22 al., 2001). Since the thorny excrescences in our experiments could have been poorly voltage-
23 clamped (at -60 mV) during the induction protocol, one or more of these channels may have
24 contributed to the rise in postsynaptic Ca^{2+} . To address this possibility, we clamped CA3
25 neurons at -80 mV, a voltage at which all VGCCs should be closed. L-type channels mediate a
26 Ca^{2+} rise induced by MF burs stimulation (Kapur et al., 2001). We therefore also added

1 nifedipine (25 μ M) to the bath solution to ensure L-type VGCCs were blocked in this experiment.
2 If L-type channels were in fact the source of the Ca^{2+} required for the putative retrograde
3 suppression, we would expect that blocking those channels would mimic the effect of BAPTA,
4 and that both control and BAPTA-dialyzed cells exhibit robust PTP. However, under these
5 recording conditions, a large difference between control and BAPTA-dialyzed cells remained
6 (**Fig. 4a**), suggesting that L-type channels do not contribute significantly to the regulation of MF-
7 PTP. We next examined the potential role of R-type and T-type VGCCs by adding 100 μ M Ni^{2+}
8 while blocking L-type VGCCs with 10 μ M nimodipine. Under these recording conditions, and
9 likely due to the blockade of presynaptic R-type channels, as previously reported (Breustedt et
10 al., 2003; Dietrich et al., 2003), MF-PTP was dampened, but the difference between low and
11 high postsynaptic Ca^{2+} buffering conditions remained (**Fig. 4b**). It is therefore unlikely that R-
12 type and T-type VGCCs in CA3 pyramidal neurons contribute significantly to the regulation of
13 MF-PTP under physiological intracellular Ca^{2+} buffer conditions.

14
15 To investigate the potential role of intracellular Ca^{2+} stores, we included cyclopiazonic acid
16 (CPA) (30 μ M) in the patch pipette to deplete Ca^{2+} from the endoplasmic reticulum. CPA led to
17 an increase in MF-PTP relative to control cells (**Fig. 4c**), suggesting that the rise in Ca^{2+}
18 required by the retrograde signal is mediated, at least partially, by intracellular stores. CPA
19 could have diffused from the recorded cell to the presynaptic terminal, reduced Pr, and thereby
20 increased the magnitude of PTP. To address this possibility, we delivered a synaptic burst (5
21 pulses, 25 Hz) to cells loaded with control solution, and those loaded with CPA. There was no
22 difference between the ratio of the fifth/first KAR-EPSC amplitude (control: 7.5 ± 1.7 ; n=5; CPA:
23 6.9 ± 1.2 ; n=5; p>0.5; data not shown), suggesting no difference in Pr. Thus, the increase in
24 PTP seen in CPA-loaded cells was likely due to depletion of postsynaptic Ca^{2+} stores. Lastly,
25 release of Ca^{2+} from internal stores can be triggered by activation of inositol 1,4,5-trisphosphate
26 receptors (IP3Rs)(Verkhratsky, 2005), a signaling pathway that has been shown to underlie

1 Ca^{2+} rises in CA3 pyramidal neurons (Kapur et al., 2001) and postsynaptic plasticity (Kwon and
2 Castillo, 2008b) at the MF-CA3 synapse. To examine whether IP3Rs played a role in the
3 suppression of MF-PTP, we included heparin (2.5 mg/mL) in the patch pipette. With IP3Rs
4 blocked, PTP was increased to a similar level as when cells were loaded with CPA (**Fig. 4d**).
5 Together, these results suggest that IP3R-triggered release from internal Ca^{2+} stores
6 contributes to the suppressive effect on PTP.

7

8 **Assessing the mechanism underlying MF-PTP suppression**

9 One way that the release of Ca^{2+} from internal stores can be triggered is via activation of group I
10 mGluRs (i.e. mGluR1 and mGluR5 subtypes). These G-protein-coupled receptors (GPCRs) are
11 likely activated during our PTP induction protocol and have been shown to mobilize Ca^{2+} stores
12 at the MF-CA3 synapse (Kapur et al., 2001). However, with the mGluR5 antagonist MPEP (4
13 μM) and the mGluR1 antagonist CPCCOEt (100 μM) in the bath solution, a large difference
14 remained between the potentiation observed in control and BAPTA-dialyzed cells (**Fig. 5a**),
15 whereas in separate experiments we found these antagonists greatly reduced the inward
16 current induced by the group I mGluR agonist DHPG (**Extended Fig. 5a**). To test for the
17 potential involvement of other GPCRs in mobilizing Ca^{2+} from internal stores (e.g. by activating
18 IP3Rs), we used GDP- β S (1 mM), a nonhydrolyzable GDP analog that interferes with G-protein
19 signaling. Including GDP- β S in the recording pipette solution had no apparent effect on the
20 retrograde suppression as we observed significantly less MF-PTP in control compared to
21 BAPTA-dialyzed cells (**Fig. 5b**). As positive control, we found that intracellularly loaded GDP- β S
22 in CA3 pyramidal neurons abolished the outward current induced by the GABA_BR agonist
23 baclofen (50 μM) (**Extended Fig. 5b**). Altogether, these results suggest that mobilization of the
24 putative retrograde signal that suppresses MF-PTP requires IP3R-mediated release of Ca^{2+}
25 from internal stores, but is independent from the activation of Group I mGluRs or other GPCR-

1 dependent signaling, although we cannot rule out the possibility that G protein-independent
2 signaling could be involved (Gerber et al., 2007).

3
4 Dendrites on postsynaptic neurons have been shown to release retrograde messengers
5 consisting of lipids, gases, peptides, growth factors, and conventional neurotransmitters
6 (Regehr et al., 2009), some of which are released by SNARE-dependent exocytosis. To test
7 whether the putative retrograde signaling suppressing MF-PTP involves vesicular release, we
8 used botulinum toxin-B (BoTX), which cleaves synaptobrevin-2, thus eliminating SNARE-
9 dependent exocytosis (Schiavo et al., 2000; Montal, 2010). Adding BoTX (5 nM) to the
10 intracellular solution did not enhance MF-PTP (**Fig. 5c**). In separate, interleaved experiments
11 that served as a positive control, and as previously reported (Lledo et al., 1998), we found that
12 loading BoTx into CA1 pyramidal neurons blocked LTP of AMPAR-mediated transmission (see
13 Methods) (**Extended Fig. 5c**). These findings argue against SNARE-dependent exocytosis in
14 mediating the putative retrograde signal involved in MF-PTP suppression.

15
16 We next examined whether lipids mediate MF-PTP suppression. For instance,
17 endocannabinoids, perhaps the most characterized retrograde signals in the brain (Kano et al.,
18 2009; Castillo et al., 2012), suppress PTP at the parallel fiber-Purkinje cell synapse in the
19 cerebellum by activating presynaptic type 1 cannabinoid receptors (Beierlein et al., 2007). To
20 test whether a different lipid signal acting as a retrograde signal, such as arachidonic acid (AA)
21 (Carta et al., 2014), or the AA metabolite 12-(S)-HPETE (Feinmark et al., 2003), could suppress
22 MF-PTP, we added a cocktail of inhibitors to the patch pipette solution in order to inhibit AA and
23 other components of lipid synthesis in the postsynaptic neuron. We included eicosatetraenoic
24 acid (ETYA; 100 μ M) and indomethacin (10 μ M) to inhibit lipoxygenases and cyclooxygenases

1 (COX 1 and 2), enzymes that catalyze the metabolism of eicosanoids and prostanoids,
2 respectively. We also added RHC-80267 (50 μ M) to inhibit diacylglycerol (DAG) lipase. With this
3 combination of lipid inhibitors in the pipette, we continued to see robust MF-PTP in BAPTA-
4 dialyzed cells, but none when the cocktail was included in control cells (**Fig. 5d**). Our results
5 suggest that the putative retrograde signal that suppressed PTP at the MF-CA3 synapse does
6 not depend on these lipid-derived pathways.

7
8 Lastly, we explored potential ways by which glutamate release was suppressed during PTP.
9 Presynaptic type 1 adenosine receptors (A1Rs) can tonically inhibit glutamate release at this
10 synapse (Moore et al., 2003) (but see Kukley et al., 2005). To test whether these receptors
11 mediate MF-PTP suppression, we used the A1R-selective antagonist DPCPX (200 nM). DPCPX
12 did not alter the robust difference in PTP observed in control vs. BAPTA-dialyzed cells (**Fig. 5e**),
13 but significantly increased the amplitude of MF KAR-EPSCs (**Extended Fig. 5d**), indicating that
14 DPCPX was active and therefore, A1Rs were not underlying the suppression of MF-PTP.
15 Glutamate release from MFs is also blocked by the activation of presynaptic group II/III mGluRs
16 (Kamiya et al., 1996). While our results using BoTX make it unlikely that these receptors were
17 targeted by glutamate released from the postsynaptic cell, glutamate could have been
18 generated from other sources (e.g. glia). However, in the presence of the group II and III mGluR
19 antagonists LY 341495 (1 μ M) and MSOP (200 μ M), respectively, the large difference between
20 control and BAPTA remained (**Fig. 5f**). These antagonists almost completely reverse the DCG-
21 IV-mediated suppression of MF transmission (**Extended Fig. 5e**). It is therefore unlikely that
22 activation of presynaptic mGluR2/3 underlies the suppression of MF-PTP.

23
24 **Strong presynaptic activity is required for retrograde suppression of glutamate release**
25 The types of activity under which retrograde suppression of transmitter release manifests could
26 have important implications for the CA3 network. We found that burst-induced facilitation,

1 measured by the ratio of the fifth KAR-EPSC amplitude to that of the first (P5/P1) in a single
2 burst (five pulses, 25 Hz), was not significantly different in control vs BAPTA conditions (**Fig.**
3 **6a**). We also examined the effect of postsynaptic Ca^{2+} buffering on low-frequency facilitation
4 (LFF), whereby single KAR-EPSCs were evoked, first during 0.1 Hz basal stimulation, and after
5 switching to 1 Hz. No difference was observed between conditions (**Fig. 6b**). Thus, for these
6 modest increases in activity, postsynaptic Ca^{2+} buffering seemed to have no impact on
7 presynaptic transmitter release. Moreover, because frequency facilitation is highly dependent on
8 the starting Pr (Zucker and Regehr, 2002; Nicoll and Schmitz, 2005; Regehr, 2012), these
9 results argue against a tonic suppression of neurotransmitter release under high postsynaptic
10 Ca^{2+} buffering conditions.

11
12 We next delivered multiple bursts in order to determine how strong the bursting paradigm must
13 be before retrograde suppression of MF-PTP is observed. To this end, we increased the
14 number of bursts while maintaining both the frequency within a burst (50 Hz), as well as
15 between bursts (2 Hz). After three bursts, synaptic responses were similar in both Ca^{2+} buffering
16 conditions (i.e. control and BAPTA), but a difference emerged after 10 bursts (**Fig. 6c**), and a
17 larger difference was also seen after increasing the number of bursts to 50. In BAPTA-dialyzed
18 cells, there was a difference between 3 vs. 10 (ANOVA, $F=21.9$; $p<0.05$; $DF=10$), 3 vs. 25
19 ($p<0.001$, $DF=10$), 3 vs. 50 ($p<0.001$, $DF=9$), 10 vs. 50 ($p<0.001$, $DF=11$), and 25 vs. 50 bursts
20 ($p<0.05$, $DF=11$). Together these data not only uncover the magnitude of MF-PTP in the
21 absence of a retrograde suppressive signal, but also show that in our BAPTA conditions, a
22 longer bursting paradigm induces stronger MF-PTP. The threshold observed with 10 bursts is
23 relatively modest, highlighting that this form of regulation could likely manifest *in vivo*.

24
25 We next examined whether stronger activation of MFs could overcome the suppressive
26 retrograde signal. To address this possibility we delivered high-frequency stimulation (HFS)

1 consisting of three trains of 100 stimuli (100 Hz within a train; trains separated by 10 seconds).

2 While a sizeable potentiation was elicited in control cells, the magnitude of MF-PTP was
3 significantly larger in conditions of high Ca^{2+} buffering (**Fig. 6d**). Thus, the putative retrograde
4 signal is strong enough to dampen the PTP evoked even by prolonged high-frequency tetanus.

5

6 It has been suggested that the MF-CA3 synapse can operate as a conditional detonator (Treves
7 and Rolls, 1992; Urban et al., 2001; Henze et al., 2002), and a recent study demonstrated that
8 MF-PTP could convert MF-CA3 synapses into full detonators (Vyleta et al., 2016). However,
9 recordings in this study –like many other voltage-clamp studies– were performed under high
10 postsynaptic Ca^{2+} buffering conditions, i.e. 10 mM EGTA in the recording pipette. We therefore
11 reassessed the role of PTP in MF detonation using physiological intracellular Ca^{2+} buffering. To
12 this end, we tested whether PTP induction facilitated the ability of a short MF burst (3 stim, 25
13 Hz) to generate action potentials in the postsynaptic CA3 pyramidal neurons loaded with either
14 0.1 mM EGTA (control) or 10 mM BAPTA. Eliciting action potentials in BAPTA neurons was
15 easier than in control neurons, which could be due to changes in excitability (Nelson et al.,
16 2003; Roussel et al., 2006). We found that the spike probability 3 min post-PTP was significantly
17 enhanced in BAPTA but not control cells (**Fig. 6e-h**). These results indicate that the contribution
18 of PTP to MF detonation can be overestimated under high postsynaptic Ca^{2+} buffer recording
19 conditions.

20

21 **DISCUSSION**

22

23 We report here that the Ca^{2+} buffering capacity of the postsynaptic neuron can significantly
24 impact presynaptically-expressed PTP at the hippocampal MF-CA3 synapse. Under normal
25 Ca^{2+} buffering capacity, as observed during non-invasive recording conditions (e.g. perforated
26 patch recording) that do not significantly alter the physiological intracellular milieu, we found that

1 a bursting induction protocol designed to mimic *in vivo* activity patterns of GCs triggered a
2 remarkably weak PTP. However, a far greater potentiation was revealed under high
3 postsynaptic Ca^{2+} buffering conditions. Remarkably, increasing the postsynaptic buffer capacity
4 had no significant effect on the basal Pr, arguing against a tonic suppression of neurotransmitter
5 release. The most parsimonious explanation for our findings is the presence of a Ca^{2+} -
6 dependent, retrograde signaling mechanism that suppresses PTP. A minimum threshold was
7 required before the phenomenon was observed, above which it operated in a wide range of
8 activity. These results point to a novel, activity-dependent form of negative feedback at the MF-
9 CA3 synapse that may significantly impact DG – CA3 information transfer.

10

11 At first glance, our findings contrast starkly with numerous studies that have reported
12 pronounced MF-PTP (for a review see Henze et al., 2000). However, most of these studies
13 elicited MF-PTP with strong repetitive stimulation (e.g. HFS) while monitoring MF transmission
14 with extracellular field recordings. Due to activation of the CA3 network, these experimental
15 conditions not only enable the recruitment of associational-commissural inputs that are
16 commonly interpreted as MF-mediated responses, but also facilitate population spike
17 contamination of (extracellularly recorded) synaptic responses (Henze et al., 2000; Nicoll and
18 Schmitz, 2005). As a result, MF-PTP magnitude can be easily overestimated. Strong MF-PTP
19 was also observed in studies that used more sensitive, single-cell recordings (see for example
20 Zalutsky and Nicoll, 1990; Maccaferri et al., 1998; Vyleta et al., 2016; Vandaël et al., 2020), but
21 here again it was typically evoked with a rather non-physiological induction protocol such as
22 HFS. Critically, many such previous studies also loaded postsynaptic neurons with 10 mM
23 EGTA, a standard concentration used in whole-cell studies, both *in vitro* and *in vivo*. Indeed, we
24 also observed striking MF-PTP in those conditions (**Fig. 2b**). Our findings therefore suggest that
25 MF-PTP is tightly controlled when afferent stimulation and postsynaptic Ca^{2+} buffering are set to
26 more physiological levels.

1
2 A rise in postsynaptic Ca^{2+} is required for most forms of retrograde signaling (Fitzsimonds and
3 Poo, 1998; Regehr et al., 2009). Consistent with this notion, MF-PTP was suppressed when the
4 postsynaptic cell was loaded with high (mimolar) concentrations of EGTA or BAPTA, or with
5 CPA or heparin, all agents that prevent a rise in intracellular Ca^{2+} . To determine the potential
6 source(s) of postsynaptic Ca^{2+} rise involved in the suppression of MF-PTP, we
7 pharmacologically interfered with these sources one by one. We found that IP3R-mediated Ca^{2+}
8 release from intracellular stores contributed to the suppression, but that Group I mGluRs and G-
9 protein-coupled signaling alone were insufficient. Importantly, however, we cannot discard
10 synergism of multiple sources leading to the full rise in postsynaptic Ca^{2+} required for retrograde
11 suppression of MF-PTP, including the contribution of VGCCs in a poorly voltage-clamped
12 postsynaptic compartment (Williams and Mitchell, 2008; Beaulieu-Laroche and Harnett, 2018).
13 Interestingly, the endogenous Ca^{2+} buffering power of CA3 pyramidal neurons is the source of
14 some debate, as some have suggested it is higher than that of CA1 cells (Wang et al., 2004),
15 while others report it is similar (Simons et al., 2009). Further complicating this matter, different
16 endogenous buffers and extrusion mechanisms create short-lived Ca^{2+} nanodomains which can
17 limit the interaction between Ca^{2+} and its substrates (Higley and Sabatini, 2008). Our data show
18 little PTP when the intracellular composition was not perturbed in perforated patch mode, and
19 robust PTP when the cell was dialyzed with a high concentration of BAPTA (**Fig. 2c**). This
20 observation would indicate that, regardless the exact endogenous buffering power of these
21 cells, it is sufficiently low to allow for the postsynaptic neuron to regulate MF-PTP.

22
23 Retrograde signaling has been proposed to influence PTP, but typically in the opposite direction
24 to our findings. For example, in the *Aplysia* sensory-motor neuron preparation, injection of
25 BAPTA into the postsynaptic cell depressed PTP (Bao et al., 1997). In the hippocampus,
26 loading CA3 pyramidal neurons with high concentrations of BAPTA (30-50 mM) curtailed PTP

1 and abolished LTP at the MF-CA3 synapse, presumably by blocking the mobilization of a
2 retrograde signal (Yeckel et al., 1999; but see Mellor and Nicoll, 2001). There is also evidence
3 that the receptor tyrosine kinase ephrin B (EphB) and its membrane-bound ligand ephrin B
4 mediate retrograde communication at MF-CA3 synapses, and that interfering with EphB/ephrin
5 B signaling inhibits both PTP and LTP at MF-CA3 synapses (Contractor et al., 2002; Armstrong
6 et al., 2006). Our findings resemble the endocannabinoid-mediated suppression of PTP at the
7 parallel fiber-Purkinje cell synapse via presynaptic type 1 cannabinoid receptors (Beierlein et al.,
8 2007). However, these receptors are not found at MF boutons in the mature brain (Marsicano
9 and Lutz, 1999; Katona et al., 2006; Hofmann et al., 2008; Caiati et al., 2012). While the identity
10 of the putative retrograde signal generated by the postsynaptic neuron remains unidentified,
11 some usual candidates (Regehr et al., 2009) could be discarded. Vesicular, SNARE-dependent
12 exocytosis was ruled out (**Fig. 5c**), indicating that the messenger is likely not a conventional
13 neurotransmitter (e.g. glutamate or GABA). Further evidence against glutamate as a retrograde
14 signaling mediating PTP suppression is the fact that this suppression remains intact after
15 blocking presynaptic group II and III mGluRs (**Fig. 5f**). Our findings also argue against the role
16 of another putative signal, nitric oxide (NO) given that its synthesis typically requires the
17 activation of NMDARs (Christopherson et al., 1999; Sattler et al., 1999), which were blocked in
18 most of our experiments. We cannot discard the possibility that PTP suppression involves
19 retrograde signaling via synaptic adhesion molecules. It is worth noting that identifying
20 endocannabinoids as the retrograde messengers mediating the well characterized
21 depolarization-induced suppression of inhibition (DSI) took a decade of work by several groups
22 (Barinaga, 2001). Future studies will have to determine the identity of the presumably non-
23 conventional retrograde signal and the presynaptic substrate responsible for curtailing PTP
24 (Regehr, 2012).

25

1 Two recent studies suggested that MF-PTP occurs *in vivo* (Vandael et al., 2020) and switches
2 MF-CA3 synapses into full detonators (Vyleta et al., 2016). However, our results indicate that
3 the impact of PTP was likely overestimated because recordings in both studies were performed
4 under high, non-physiological Ca^{2+} buffering conditions (e.g. 10 mM EGTA). PTP has also been
5 reported at MF to inhibitory interneuron synapses (Alle et al., 2001; Mori et al., 2007). Given that
6 MFs make 10 times as many contacts onto inhibitory interneurons as onto CA3 pyramidal cells
7 (Acsady et al., 1998), PTP at MF to interneuron synapses, by presumably activating an
8 inhibitory network, could control the activity of GCs (feed-back inhibition) and detonation of CA3
9 pyramidal neurons (feed-forward inhibition) (Lawrence and McBain, 2003). However, unlike PTP
10 at MF-CA3 synapses, postsynaptic Ca^{2+} buffering had no impact on PTP magnitude at MF to
11 basket cells synapses in the DG, with similarly robust PTP when the interneuron was loaded
12 with 0.1 mM EGTA or 10 mM BAPTA (Alle et al., 2001). Thus, although PTP is observed at
13 distinct MF synapses, the retrograde suppression we report in the present study seems to be
14 unique to the MF-CA3 pyramidal cell synapse.

15
16 Relatively strong GC burst activity is needed for engaging suppression of MF-PTP, and the
17 magnitude of this suppression does not seem to be overcome by stronger presynaptic activity
18 (**Fig. 6c**). Thus, PTP suppression may serve as a powerful mechanism of controlling DG-CA3
19 information transfer following repetitive bursts of GC activity that normally occur during
20 exploratory behaviors (Henze et al., 2002; Pernia-Andrade and Jonas, 2014; Diamantaki et al.,
21 2016; GoodSmith et al., 2017; Senzai and Buzsaki, 2017). Left unchecked, MF-PTP could
22 indirectly lead to runaway activity of the CA3 network and facilitate epileptic activity. Lastly,
23 while the generalizability of PTP suppression remains untested, future studies will be required to
24 determine whether Ca^{2+} indicators widely used *in vitro* and *in vivo* throughout the brain may
25 promote a similar suppression of presynaptic function.

26

1

2

3

4 Abbott LF, Regehr WG (2004) Synaptic computation. *Nature* 431:796-803.

5 Acsady L, Kamondi A, Sik A, Freund T, Buzsaki G (1998) GABAergic cells are the major

6 postsynaptic targets of mossy fibers in the rat hippocampus. *J Neurosci* 18:3386-3403.

7 Alle H, Jonas P, Geiger JR (2001) PTP and LTP at a hippocampal mossy fiber-interneuron

8 synapse. *Proc Natl Acad Sci U S A* 98:14708-14713.

9 Armstrong JN, Saganich MJ, Xu NJ, Henkemeyer M, Heinemann SF, Contractor A (2006) B-

10 ephrin reverse signaling is required for NMDA-independent long-term potentiation of

11 mossy fibers in the hippocampus. *J Neurosci* 26:3474-3481.

12 Bao JX, Kandel ER, Hawkins RD (1997) Involvement of pre- and postsynaptic mechanisms in

13 posttetanic potentiation at Aplysia synapses. *Science* 275:969-973.

14 Barinaga M (2001) How Cannabinoids Work in the Brain. *Science* 291:2530-2531.

15 Beaulieu-Laroche L, Harnett MT (2018) Dendritic Spines Prevent Synaptic Voltage Clamp.

16 *Neuron* 97:75-82 e73.

17 Beierlein M, Fioravante D, Regehr WG (2007) Differential expression of posttetanic potentiation

18 and retrograde signaling mediate target-dependent short-term synaptic plasticity. *Neuron*

19 54:949-959.

20 Breustedt J, Vogt KE, Miller RJ, Nicoll RA, Schmitz D (2003) Alpha1E-containing Ca²⁺

21 channels are involved in synaptic plasticity. *Proc Natl Acad Sci U S A* 100:12450-12455.

22 Caiati MD, Sivakumaran S, Lanore F, Mulle C, Richard E, Verrier D, Marsicano G, Miles R,

23 Cherubini E (2012) Developmental regulation of CB1-mediated spike-time dependent

24 depression at immature mossy fiber-CA3 synapses. *Scientific Reports* 2.

25 Carta M, Lanore F, Rebola N, Szabo Z, Da Silva SV, Lourenco J, Verraes A, Nadler A, Schultz

26 C, Blanchet C, Mulle C (2014) Membrane lipids tune synaptic transmission by direct

27 modulation of presynaptic potassium channels. *Neuron* 81:787-799.

28 Castillo PE, Malenka RC, Nicoll RA (1997) Kainate receptors mediate a slow postsynaptic

29 current in hippocampal CA3 neurons. *Nature* 388:182-186.

30 Castillo PE, Younts TJ, Chavez AE, Hashimotodani Y (2012) Endocannabinoid signaling and

31 synaptic function. *Neuron* 76:70-81.

32 Christopherson KS, Hillier BJ, Lim WA, Bredt DS (1999) PSD-95 assembles a ternary complex

33 with the N-methyl-D-aspartic acid receptor and a bivalent neuronal NO synthase PDZ

34 domain. *J Biol Chem* 274:27467-27473.

35 Claiborne BJ, Xiang Z, Brown TH (1993) Hippocampal circuitry complicates analysis of long-

36 term potentiation in mossy fiber synapses. *Hippocampus* 3:115-121.

37 Contractor A, Rogers C, Maron C, Henkemeyer M, Swanson GT, Heinemann SF (2002) Trans-

38 synaptic Eph receptor-ephrin signaling in hippocampal mossy fiber LTP. *Science*

39 296:1864-1869.

40 Diamantaki M, Frey M, Berens P, Preston-Ferrer P, Burgalossi A (2016) Sparse activity of

41 identified dentate granule cells during spatial exploration. *Elife* 5.

42 Dietrich D, Kirschstein T, Kukley M, Pereverzev A, von der Brelie C, Schneider T, Beck H

43 (2003) Functional specialization of presynaptic Cav2.3 Ca²⁺ channels. *Neuron* 39:483-

44 496.

45 Feinmark SJ, Begum R, Tsvetkov E, Goussakov I, Funk CD, Siegelbaum SA, Bolshakov VY

46 (2003) 12-lipoxygenase metabolites of arachidonic acid mediate metabotropic glutamate

1 receptor-dependent long-term depression at hippocampal CA3-CA1 synapses. *J Neurosci*
2 23:11427-11435.

3 Fitzsimonds RM, Poo MM (1998) Retrograde signaling in the development and modification of
4 synapses. *Physiol Rev* 78:143-170.

5 Gerber U, Gee CE, Benquet P (2007) Metabotropic glutamate receptors: intracellular signaling
6 pathways. *Curr Opin Pharmacol* 7:56-61.

7 GoodSmith D, Chen X, Wang C, Kim SH, Song H, Burgalossi A, Christian KM, Knierim JJ
8 (2017) Spatial Representations of Granule Cells and Mossy Cells of the Dentate Gyrus.
9 *Neuron* 93:677-690 e675.

10 Griffith WH (1990) Voltage-clamp analysis of posttetanic potentiation of the mossy fiber to CA3
11 synapse in hippocampus. *J Neurophysiol* 63:491-501.

12 Henze DA, Urban NN, Barrionuevo G (2000) The multifarious hippocampal mossy fiber
13 pathway: a review. *Neuroscience* 98:407-427.

14 Henze DA, Wittner L, Buzsaki G (2002) Single granule cells reliably discharge targets in the
15 hippocampal CA3 network in vivo. *Nat Neurosci* 5:790-795.

16 Higley MJ, Sabatini BL (2008) Calcium signaling in dendrites and spines: practical and
17 functional considerations. *Neuron* 59:902-913.

18 Hofmann ME, Nahir B, Frazier CJ (2008) Excitatory afferents to CA3 pyramidal cells display
19 differential sensitivity to CB1 dependent inhibition of synaptic transmission.
20 *Neuropharmacology* 55:1140-1146.

21 Jonas P, Major G, Sakmann B (1993) Quantal components of unitary EPSCs at the mossy fibre
22 synapse on CA3 pyramidal cells of rat hippocampus. *J Physiol* 472:615-663.

23 Kamiya H, Shinozaki H, Yamamoto C (1996) Activation of metabotropic glutamate receptor
24 type 2/3 suppresses transmission at rat hippocampal mossy fibre synapses. *J Physiol* 493 (Pt 2):447-455.

25 Kano M, Ohno-Shosaku T, Hashimotodani Y, Uchigashima M, Watanabe M (2009)
26 Endocannabinoid-mediated control of synaptic transmission. *Physiol Rev* 89:309-380.

27 Kapur A, Yeckel M, Johnston D (2001) Hippocampal mossy fiber activity evokes Ca²⁺ release
28 in CA3 pyramidal neurons via a metabotropic glutamate receptor pathway. *Neuroscience*
29 107:59-69.

30 Katona I, Urban GM, Wallace M, Ledent C, Jung KM, Piomelli D, Mackie K, Freund TF (2006)
31 Molecular composition of the endocannabinoid system at glutamatergic synapses. *J
32 Neurosci* 26:5628-5637.

33 Kukley M, Schwan M, Fredholm BB, Dietrich D (2005) The role of extracellular adenosine in
34 regulating mossy fiber synaptic plasticity. *J Neurosci* 25:2832-2837.

35 Kwon HB, Castillo PE (2008a) Role of glutamate autoreceptors at hippocampal mossy fiber
36 synapses. *Neuron* 60:1082-1094.

37 Kwon HB, Castillo PE (2008b) Long-term potentiation selectively expressed by NMDA
38 receptors at hippocampal mossy fiber synapses. *Neuron* 57:108-120.

39 Lawrence JJ, McBain CJ (2003) Interneuron diversity series: containing the detonation--
40 feedforward inhibition in the CA3 hippocampus. *Trends Neurosci* 26:631-640.

41 Lledo PM, Zhang X, Sudhof TC, Malenka RC, Nicoll RA (1998) Postsynaptic membrane fusion
42 and long-term potentiation. *Science* 279:399-403.

43 Maccaferri G, Toth K, McBain CJ (1998) Target-specific expression of presynaptic mossy fiber
44 plasticity. *Science* 279:1368-1370.

1 Marsicano G, Lutz B (1999) Expression of the cannabinoid receptor CB1 in distinct neuronal
2 subpopulations in the adult mouse forebrain. *Eur J Neurosci* 11:4213-4225.

3 Mellor J, Nicoll RA (2001) Hippocampal mossy fiber LTP is independent of postsynaptic
4 calcium. *Nat Neurosci* 4:125-126.

5 Montal M (2010) Botulinum Neurotoxin: A Marvel of Protein Design. *Annual Review of
6 Biochemistry*, Vol 79 79:591-617.

7 Moore KA, Nicoll RA, Schmitz D (2003) Adenosine gates synaptic plasticity at hippocampal
8 mossy fiber synapses. *Proc Natl Acad Sci U S A* 100:14397-14402.

9 Mori M, Gahwiler BH, Gerber U (2007) Recruitment of an inhibitory hippocampal network after
10 bursting in a single granule cell. *Proc Natl Acad Sci U S A* 104:7640-7645.

11 Nelson AB, Krispel CM, Sekirnjak C, du Lac S (2003) Long-lasting increases in intrinsic
12 excitability triggered by inhibition. *Neuron* 40:609-620.

13 Nicoll RA, Schmitz D (2005) Synaptic plasticity at hippocampal mossy fibre synapses. *Nat Rev
14 Neurosci* 6:863-876.

15 Pernia-Andrade AJ, Jonas P (2014) Theta-gamma-modulated synaptic currents in hippocampal
16 granule cells in vivo define a mechanism for network oscillations. *Neuron* 81:140-152.

17 Regehr WG (2012) Short-Term Presynaptic Plasticity. *Cold Spring Harbor Perspectives in
18 Biology* 4.

19 Regehr WG, Delaney KR, Tank DW (1994) The role of presynaptic calcium in short-term
20 enhancement at the hippocampal mossy fiber synapse. *J Neurosci* 14:523-537.

21 Regehr WG, Carey MR, Best AR (2009) Activity-dependent regulation of synapses by
22 retrograde messengers. *Neuron* 63:154-170.

23 Reid CA, Fabian-Fine R, Fine A (2001) Postsynaptic calcium transients evoked by activation of
24 individual hippocampal mossy fiber synapses. *J Neurosci* 21:2206-2214.

25 Roussel C, Erneux T, Schiffmann SN, Gall D (2006) Modulation of neuronal excitability by
26 intracellular calcium buffering: from spiking to bursting. *Cell Calcium* 39:455-466.

27 Salin PA, Scanziani M, Malenka RC, Nicoll RA (1996) Distinct short-term plasticity at two
28 excitatory synapses in the hippocampus. *Proc Natl Acad Sci U S A* 93:13304-13309.

29 Sattler R, Xiong Z, Lu WY, Hafner M, MacDonald JF, Tymianski M (1999) Specific coupling of
30 NMDA receptor activation to nitric oxide neurotoxicity by PSD-95 protein. *Science*
31 284:1845-1848.

32 Scanziani M, Salin PA, Vogt KE, Malenka RC, Nicoll RA (1997) Use-dependent increases in
33 glutamate concentration activate presynaptic metabotropic glutamate receptors. *Nature*
34 385:630-634.

35 Schiavo G, Matteoli M, Montecucco C (2000) Neurotoxins affecting neuroexocytosis. *Physiol
36 Rev* 80:717-766.

37 Senzai Y, Buzsaki G (2017) Physiological Properties and Behavioral Correlates of Hippocampal
38 Granule Cells and Mossy Cells. *Neuron* 93:691-704 e695.

39 Simons SB, Escobedo Y, Yasuda R, Dudek SM (2009) Regional differences in hippocampal
40 calcium handling provide a cellular mechanism for limiting plasticity. *Proc Natl Acad Sci
41 U S A* 106:14080-14084.

42 Toth K, Suares G, Lawrence JJ, Philips-Tansey E, McBain CJ (2000) Differential mechanisms of
43 transmission at three types of mossy fiber synapse. *J Neurosci* 20:8279-8289.

44 Treves A, Rolls ET (1992) Computational constraints suggest the need for two distinct input
45 systems to the hippocampal CA3 network. *Hippocampus* 2:189-199.

1 Urban NN, Henze DA, Barrientos G (2001) Revisiting the role of the hippocampal mossy fiber
2 synapse. *Hippocampus* 11:408-417.

3 Vanda D, Borges-Merjane C, Zhang X, Jonas P (2020) Short-Term Plasticity at Hippocampal
4 Mossy Fiber Synapses Is Induced by Natural Activity Patterns and Associated with
5 Vesicle Pool Engram Formation. *Neuron* 107:509-521 e507.

6 Verkhratsky A (2005) Physiology and pathophysiology of the calcium store in the endoplasmic
7 reticulum of neurons. *Physiol Rev* 85:201-279.

8 Vyleta NP, Borges-Merjane C, Jonas P (2016) Plasticity-dependent, full detonation at
9 hippocampal mossy fiber-CA3 pyramidal neuron synapses. *Elife* 5.

10 Wang J, Yeckel MF, Johnston D, Zucker RS (2004) Photolysis of postsynaptic caged Ca²⁺ can
11 potentiate and depress mossy fiber synaptic responses in rat hippocampal CA3 pyramidal
12 neurons. *J Neurophysiol* 91:1596-1607.

13 Weisskopf MG, Nicoll RA (1995) Presynaptic changes during mossy fibre LTP revealed by
14 NMDA receptor-mediated synaptic responses. *Nature* 376:256-259.

15 Williams SR, Mitchell SJ (2008) Direct measurement of somatic voltage clamp errors in central
16 neurons. *Nat Neurosci* 11:790-798.

17 Yeckel MF, Kapur A, Johnston D (1999) Multiple forms of LTP in hippocampal CA3 neurons
18 use a common postsynaptic mechanism. *Nat Neurosci* 2:625-633.

19 Zalutsky RA, Nicoll RA (1990) Comparison of two forms of long-term potentiation in single
20 hippocampal neurons. *Science* 248:1619-1624.

21 Zucker RS, Regehr WG (2002) Short-term synaptic plasticity. *Annu Rev Physiol* 64:355-405.

22
23

1 **Figure Legends**

2

3 **Figure 1. High postsynaptic Ca^{2+} buffering selectively enhances post-tetanic potentiation**

4 **at the MF-CA3 synapse.** (a) Summary data showing the effect of loading the patch pipette with

5 10 mM BAPTA on PTP of AMPAR-mediated MF-responses compared to control condition (0.1

6 mM EGTA) (Control: $125 \pm 52\%$ of baseline; n=6; BAPTA: $347 \pm 84\%$; n=6; Control vs. BAPTA:

7 $p < 0.05$). Experiments were performed at 32°C , $V_h = -60$ mV, with only a low concentration of

8 the AMPAR selective antagonist GYKI-53655 (1 μM), and the bursting paradigm was performed

9 in current-clamp mode. AMPAR-EPSCs were evoked with bulk stimulation in the GC layer. At

10 the end of the experiments, DCG-IV (1 μM) was added to the bath to verify that the synaptic

11 responses were mediated by MF activation. PTP is quantified as the average of the EPSCs

12 during the first three minutes post-induction vs the three minutes prior induction. Representative

13 traces (*top*) and time-course summary plot (*bottom*). (b) Summary data of experiments in which

14 the same bursting paradigm was performed at the neighboring associational-commissural (CA3-

15 CA3) synapse. Note no difference between control and BAPTA-dialyzed cells (Control: $101 \pm$

16 6%; n=5; BAPTA: $95 \pm 3\%$; n=7; Control vs. BAPTA: $p > 0.3$). NBQX was used at the end of the

17 experiments to confirm AMPAR-mediated responses. (c) PTP assessed by minimal stimulation

18 of MFs while monitoring AMPAR-EPSCs in the absence of drugs in the bath. PTP was induced

19 in current-clamp mode. *Left*, representative traces showing successes (black) and failures

20 (grey). *Right*, summary data showing MF-PTP elicited with minimal stimulation in control and

21 BAPTA-dialyzed cells (Control: 112 ± 27 of baseline; n=6; BAPTA: 354 ± 82 ; n=6; Control vs.

22 BAPTA: $p < 0.05$). (d) PPR was not affected by intracellular 10 mM BAPTA loading (Control: 2.5

23 ± 0.18 ; n=10; BAPTA: 2.3 ± 0.17 ; n=6; Control vs. BAPTA: $p > 0.5$). Number of cells are

24 indicated between brackets.

25 Here and in all figures, data are presented as mean \pm SEM; representative traces correspond to

26 the time points indicated by numbers on the time-course plots.

1
2 **Figure 2. Weak MF-PTP of KAR-mediated transmission under physiological postsynaptic**
3 **Ca²⁺ buffering recording conditions. (a)** Summary data showing the effect of 10 mM BAPTA
4 on MF-PTP (Control: 115 ± 6%; n=6; BAPTA: 203 ± 14%; n=7; Control vs. BAPTA: p<0.001).
5 **(b)** Summary data for Control vs 10 mM EGTA (Control: 122 ± 13%, n=7; 10 mM EGTA: 196 ±
6 17% of baseline, n=6; Control vs 10 mM EGTA p<0.01). **(c) Left,** Summary effect when 10 mM
7 BAPTA was included in the recording pipette, in whole-cell vs. perforated-patch configuration
8 (BAPTA perforated patch: 138 ± 11%; n=7; BAPTA whole cell: 226 ± 11%; n=4; BAPTA
9 perforated patch vs. BAPTA whole-cell: p<0.001). **Right,** EPSPs from representative
10 experiments.

11
12 **Figure 3. Enhanced MF-PTP by high postsynaptic Ca²⁺ buffering capacity is**
13 **presynaptically expressed. (a)** Summary data showing the effect of 25 bursts on NMDAR-
14 mediated EPSCs ($V_H = -50$ mV), when CA3 neurons were dialyzed with control vs BAPTA
15 intracellular solution (control: 102 ± 11% of baseline; n=5; BAPTA: 191 ± 23%; n=7; control vs.
16 BAPTA: p<0.05). **(b)** Summary plot of the AMPAR-mediated MF response after the bursting
17 paradigm, in control vs. BAPTA conditions (control: 135 ± 17%; n=6; BAPTA: 223 ± 16%; n=7;
18 control vs. BAPTA: p<0.01). **(c)** KAR PPR was monitored by delivering two pulses (40 ms inter-
19 stimulus interval). **Top,** Averaged traces from representative experiments, before and after
20 bursting, and summary plot of the first EPSC amplitude in control vs. BAPTA solutions. **Bottom,**
21 Summary of PPR time course as normalized to the three minutes before the bursting paradigm.
22 Same cells as in top panel (Control: 80 ± 8%; n=7; BAPTA: 37 ± 5%; n=6; control vs. BAPTA:
23 p<0.01).

24
25 **Figure 4. Suppression of MF-PTP depends on internal Ca²⁺ stores. (a)** Summary effect of
26 voltage-clamping cells at -80 mV with 25 μM nifedipine in the bath in control and BAPTA-

1 dialyzed cells (Control: $138 \pm 3\%$; n=5; BAPTA: $209 \pm 20\%$; n=5; control vs. BAPTA: p<0.01).
2 (b) Summary effect of adding 100 μM Ni^{2+} and 10 μM nimodipine to the bath (Control: $110 \pm 14\%$;
3 n=9; BAPTA: $151 \pm 9\%$; n=8; control vs. BAPTA: p < 0.05). (c) Summary effect of including
4 cyclopiazonic acid (CPA) in the patch pipette (Control: $112 \pm 6\%$; n=4; CPA: $156 \pm 16\%$; n=5;
5 Control vs CPA: p<0.05). (d) Summary effect of including heparin in the recording pipette to
6 block IP3Rs (Control: $112 \pm 2\%$; n=5; heparin: $157 \pm 17\%$; n=5; Control vs heparin: p<0.05).
7

8 **Figure 5. Assessing the mechanism underlying MF-PTP suppression.** (a) Summary of data
9 of MF-PTP under control (0.1 mM EGTA) and high intracellular buffering conditions (10 mM
10 BAPTA) in the presence of the Group I mGluR antagonists MPEP and CPCCOEt (Control: $122 \pm 6\%$; n=6; BAPTA: $208 \pm 28\%$; n=6; control vs. BAPTA: p<0.05). (b) Summary data of
12 experiments in which control and BAPTA cells were dialyzed with GDP- β S (Control-GDP- β S: $106 \pm 13\%$; n=5; BAPTA-GDP- β S: $161 \pm 17\%$; n=5; control-GDP- β S vs. BAPTA-GDP- β S: p<0.05). (c) Cells dialyzed with botulinum toxin B (BoTX) did not exhibit any more PTP than
15 interleaved controls without BoTX (BoTX included in control solution: $116 \pm 2\%$; n=5; BAPTA
without BoTX: $189 \pm 16\%$; n=5; control-BoTX vs. BAPTA: p<0.01). (d) Summary data when a
17 cocktail of lipid blockers (ETYA, indomethacin, and RHC-80267) was included in the intracellular
18 recording solution (Control: $105 \pm 6\%$ of baseline; n=6; BAPTA: $220 \pm 21\%$; n=4; control vs.
19 BAPTA: p<0.001). (e) Summary data showing no PTP in control cells after bursting paradigm in
20 the presence of the adenosine 1 receptor antagonist DPCPX, whereas robust PTP observed in
21 BAPTA-dialyzed cells (Control: $104 \pm 3\%$; n=5; BAPTA: $191 \pm 7\%$; n=4; control vs. BAPTA: p<0.001). (f) Summary data showing the effect of bursting paradigm in control and BAPTA-
23 dialyzed cells in the presence of the Group II and III mGluR antagonists LY-341495 and MSOP
24 (Control: $121 \pm 10\%$; n=6; BAPTA: $201 \pm 10\%$; n=4; control vs. BAPTA: p<0.001).
25

1 **Figure 6. MF-PTP suppression under different patterns of activity. (a)** Five pulses were
2 delivered to MFs for control and BAPTA-dialyzed cells, and the ratio of the fifth KAR-EPSC to
3 the first was taken (P5/P1 control: 6.0 ± 0.7 ; n=12; P5/P1 BAPTA: 6.5 ± 0.9 ; n=13; control vs.
4 BAPTA: p>0.5). Traces normalized to the amplitude of first EPSC. **(b)** Summary data showing
5 effect of switching basal stimulation frequency from 0.1 to 1.0 Hz in control vs. BAPTA-dialyzed
6 cells (LFF control: $341 \pm 73\%$ of baseline; n=6; LFF BAPTA: $358 \pm 59\%$; n=6; control vs.
7 BAPTA: p>0.5). Insets: superimposed traces taken at 0.1 and 1.0 Hz. Calibration bars: 40 pA
8 and 40 ms. **(c)** Summary data showing the suppressive effect on MF-PTP induced by different
9 number of bursts. Three bursts, control: $101 \pm 5\%$ of baseline; n=7; BAPTA: $102 \pm 4\%$; n=5
10 (control vs. BAPTA: p>0.5). Ten bursts, control: $121 \pm 7\%$ of baseline; n=8; BAPTA: $167 \pm 14\%$;
11 n=7 (control vs. BAPTA: p<0.01). Twenty-five bursts: control: $115 \pm 6\%$ of baseline; n=7;
12 BAPTA: $203 \pm 14\%$; n=7 (control vs. BAPTA: p<0.001). Fifty bursts: control: $147 \pm 10\%$ of
13 baseline; n=8; BAPTA: $264 \pm 15\%$; n=6 (control vs. BAPTA: p<0.001). **(d)** Effect of high
14 frequency stimulation (HFS; 100 pulses at 100 Hz, x3) on MF KAR-EPSCs, with or without
15 BAPTA in the patch pipette (Control: $181 \pm 20\%$ of baseline; n=7; BAPTA: $282 \pm 24\%$; n=5;
16 control vs. BAPTA: p<0.01). **(e-h)** Effects of MF-PTP on CA3 pyramidal neuron firing induced by
17 MF bursting stimulation. No drugs were added to the bath .Control cells loaded with 0.1 mM
18 EGTA (e,f) showed little-to-no action potentials before and after PTP (Baseline: $0 \pm 0\%$; n=6;
19 PTP: $2 \pm 2\%$; n=6; baseline vs. PTP: p > 0.4, Mann-Whitney), whereas in cells loaded with 10
20 mM BAPTA (g,h) PTP enhanced the probability of firing action potentials (baseline: $27 \pm 9\%$;
21 n=6; PTP: $42 \pm 11\%$; n=6; baseline vs. PTP: p < 0.005, paired t-test).

22

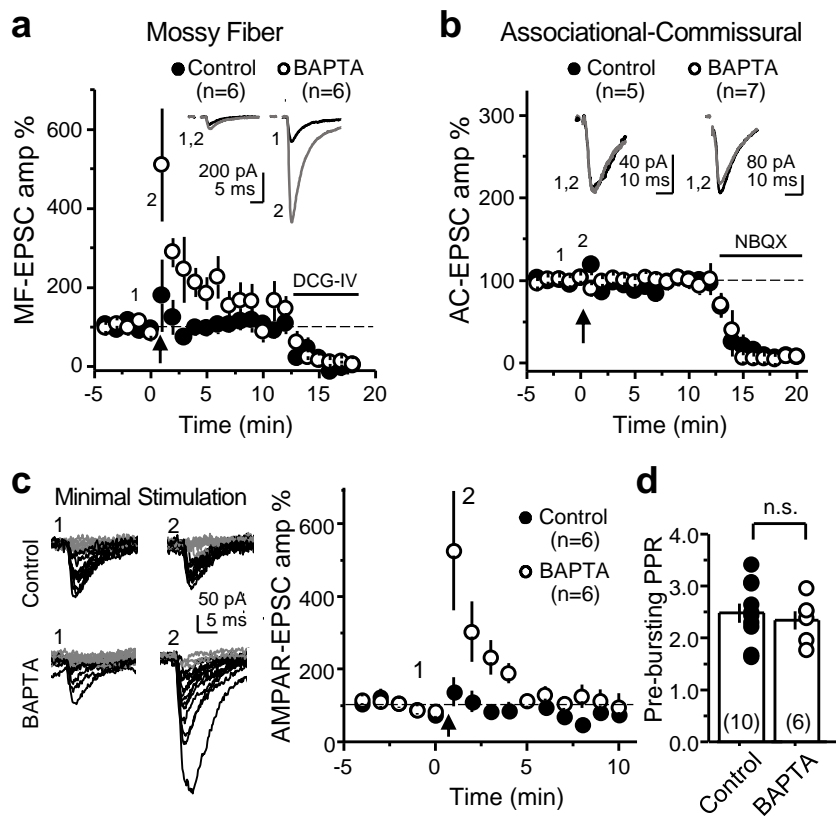


Figure 1. High postsynaptic Ca^{2+} buffering selectively enhances post-tetanic potentiation at the MF-CA3 synapse.

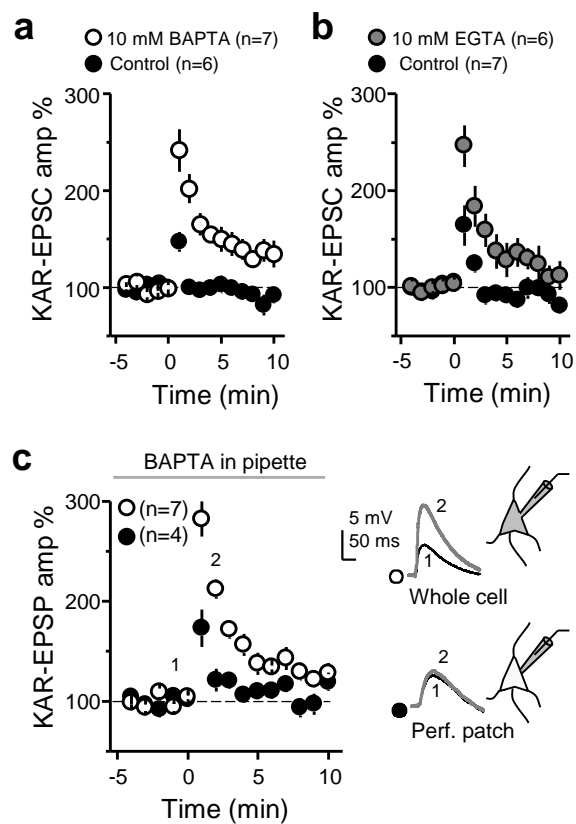


Figure 2. Weak MF-PTP of KAR-mediated transmission under physiological postsynaptic Ca^{2+} buffering recording conditions.

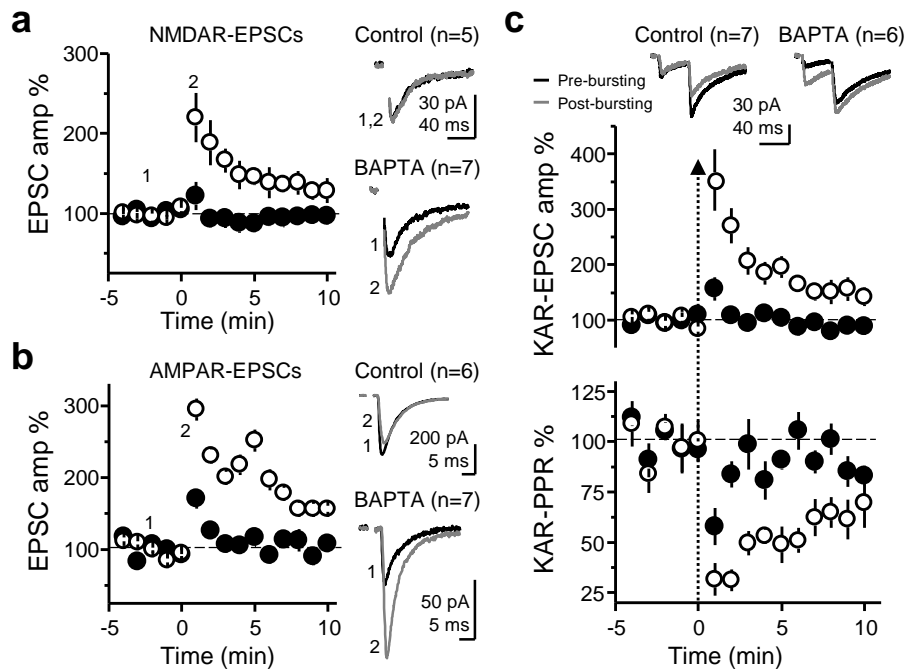


Figure 3. Enhanced MF-PTP by high postsynaptic Ca^{2+} buffering capacity is presynaptically expressed.

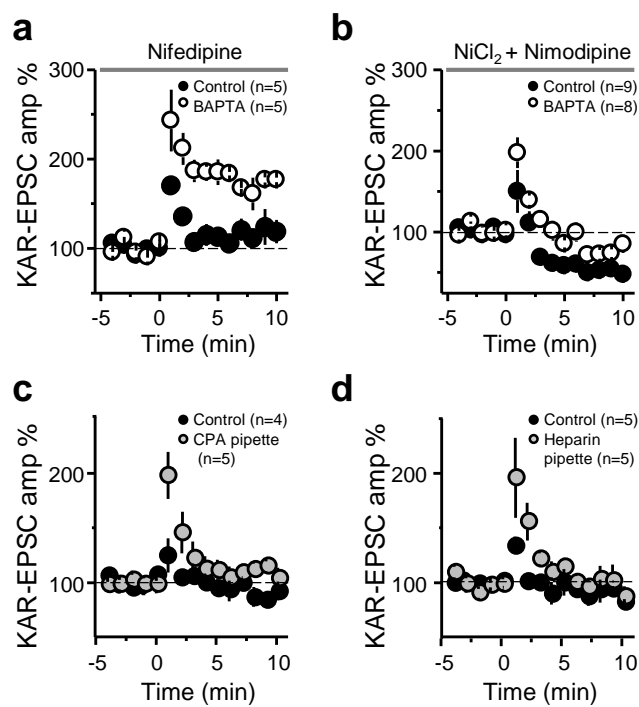


Figure 4. Suppression of MF-PTP depends on internal Ca^{2+} stores.

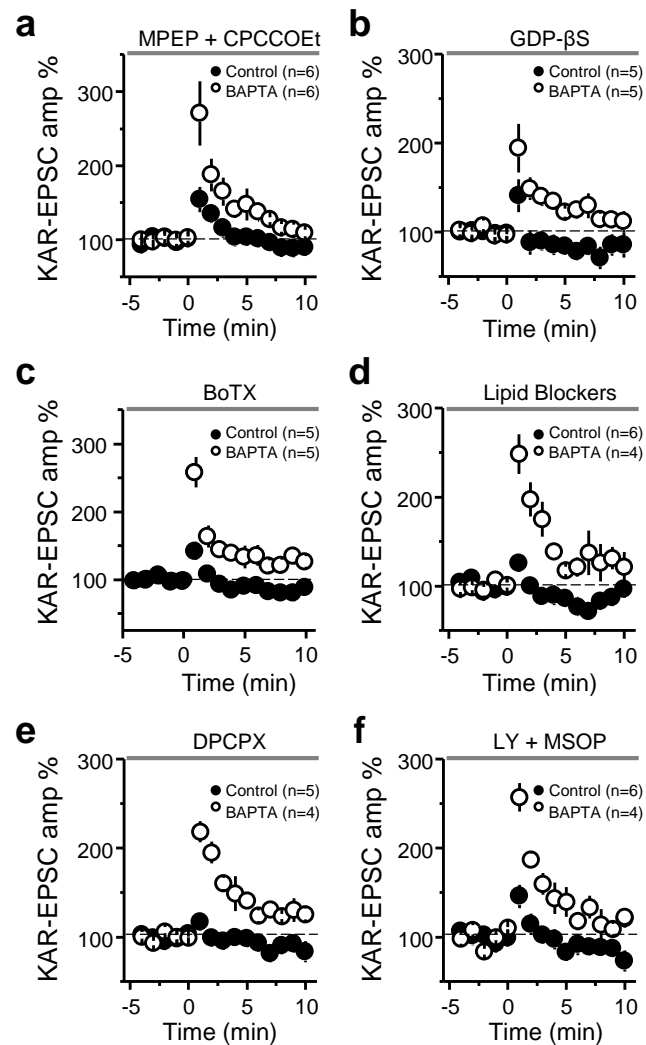


Figure 5. Assessing the mechanism underlying MF-PTP suppression.

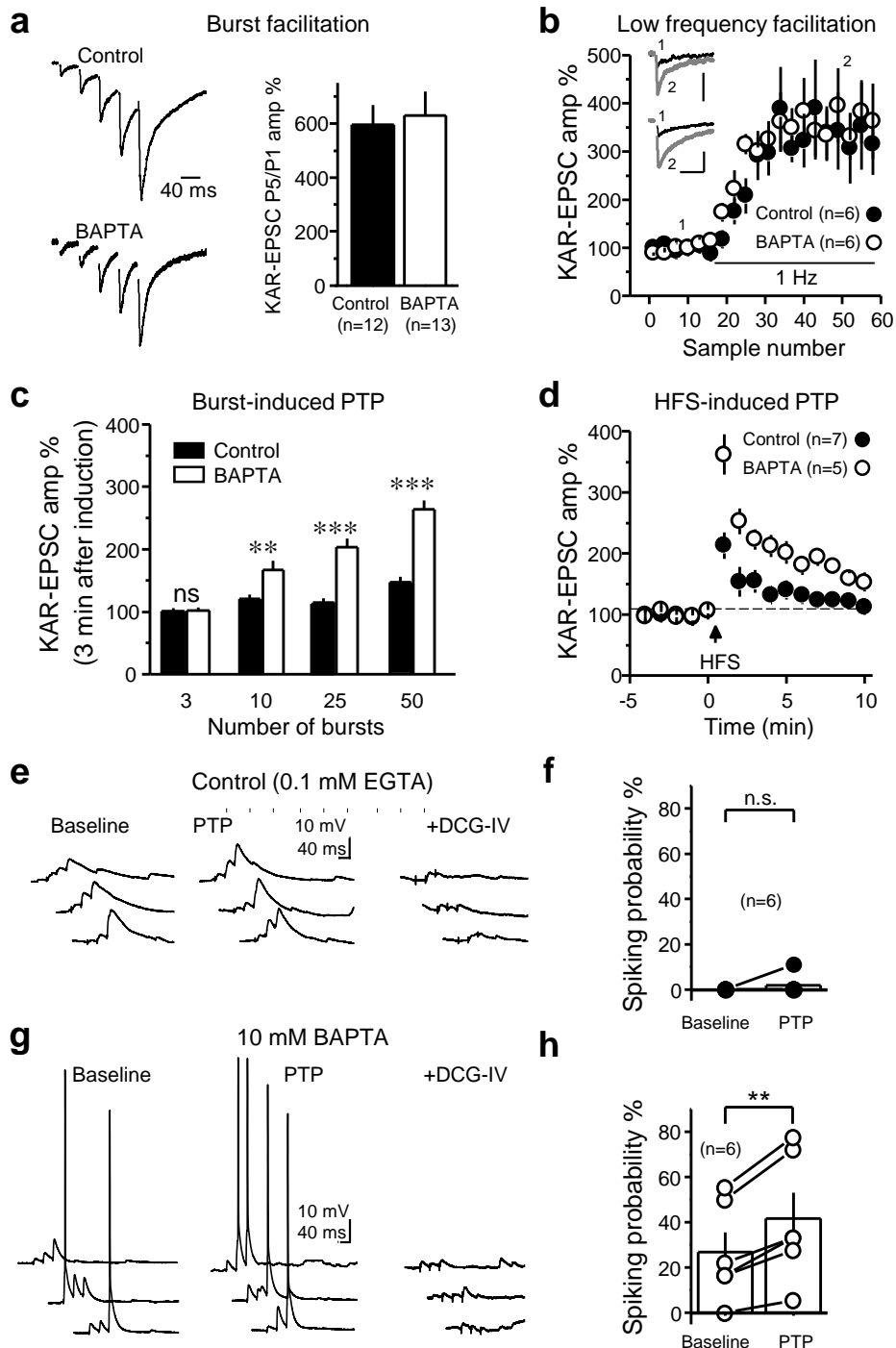
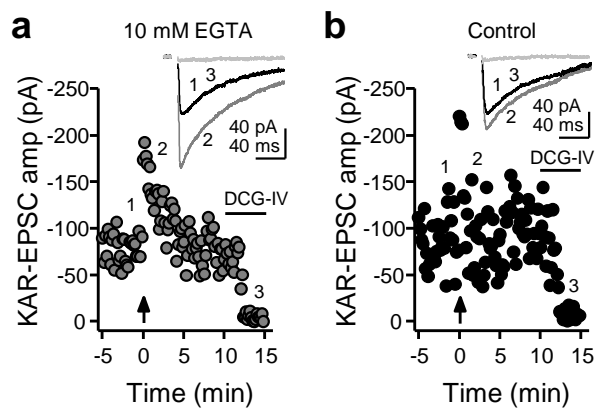
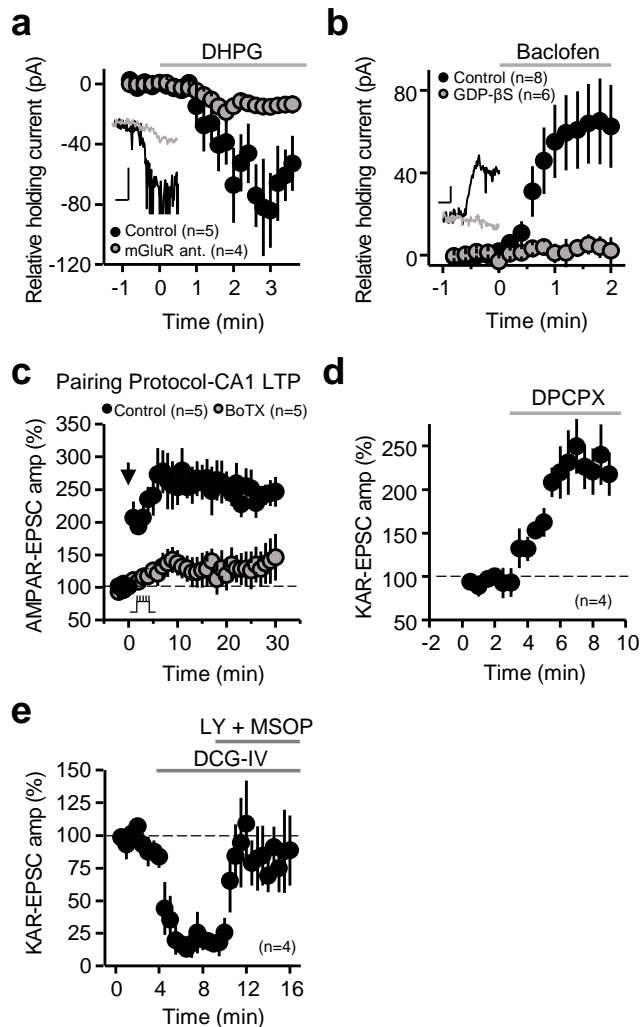


Figure 6. MF-PTP suppression under different patterns of activity.



Extended Figure 2. (a) Representative experiment in which the recording pipette solution contained 10 mM EGTA. KAR-EPSC traces, which correspond to the numbers in the time course plot below, are shown above. DCG-IV (1 μ M) was added at the end of the experiment. (b) Representative experiment in which the pipette solution contained 0.1 mM EGTA (Control). Note suppression of PTP relative to (a).



Extended Figure 5 (a) Bath application of the group I mGluR agonist DHPG (50 μ M) caused an inward current, was significantly reduced in the presence of the group I mGluR antagonists MPEP/CPCCOEt. (Control: 55 \pm 11 pA; n=5; MPEP/CPCCOEt: 14 \pm 5 pA; n=4; control vs. antagonists: p<0.05). Inset: superimposed traces in control and in the presence of MPEP/CPCCOEt. Calibration bars: 40 pA, 1 min. (b) The outward current induced by bath application of the GABA_B agonist baclofen was abolished by intracellular loading of GDP- β S (Control: 61 \pm 19 pA; n=8; GDP- β S: 3 \pm 6 pA; n=6; Control vs. GDP- β S: p<0.05). Inset: superimposed representative traces in control cells (black) and cells loaded with GDP- β S. Calibration bars: 40 pA, 1 min. (c) Loading BoTX in CA1 pyramidal neurons blocked LTP of AMPAR-mediated transmission (Control: 240 \pm 18% of baseline; n=5; BoTX: 137 \pm 30%; n=5; Control vs. BoTX: p<0.05). LTP was generated using a pairing protocol of postsynaptic depolarization (from V_H = -60 to 0 mV) for three minutes, and stimulating the Schaffer collaterals with 180 pulses (2 Hz). (d) Positive control showing the immediate potentiating effect of 200 nM DPCPX (221 \pm 25% of baseline, n=4; p<0.01). (e) The suppression of MF-mediated responses by 1 μ M DCG-IV bath application was reversed by the antagonists LY341495 (1 μ M) and MSOP (200 μ M) (90 \pm 24% of original baseline; n=4).